Contribution from the Department of Chemistry and Biochemistry, University of California, Los Angeles, California 90024

Synthesis and Characterization of Edge-Double-Bridged $Ru_3(\mu\text{-H},\mu\text{-X})(CO)_{10}$ (X = Cl, Br, I) and Face-Triple-Bridged $Ru_3(\mu\text{-H},\mu_3\text{-I})(CO)_9$. Crystal and Molecular Structure of $Ru_3(\mu\text{-H},\mu\text{-Br})(CO)_{10}$, $Ru_3(\mu\text{-I})_2(CO)_{10}$, and $Ru_3(\mu\text{-H},\mu_3\text{-I})(CO)_9$

CARSTEN E. KAMPE, NEIL M. BOAG, CAROLYN B. KNOBLER, and HERBERT D. KAESZ*

Received June 21, 1983

Reaction of $Ru_3(CO)_{12}$ with trimethylamine *N*-oxide at 0 °C in the presence of an alkali halide (LiCl, LiBr, or NaI) followed by protonation with $HBF_4 \cdot 2Et_2O$ yields the edge-double-bridged complexes $Ru_3(\mu\text{-H},\mu\text{-X})(CO)_{10}$ (X = Cl (**1**), Br (**2**), I (**3**)); small quantities of the complexes $Ru_3(\mu\text{-X})_2(CO)_{10}$ (X = Br (**4**), I (**5**)) are also observed. For X = I, the additional compound $Ru_3(\mu\text{-H},\mu_3\text{-I})(CO)_9$ (**6**) is obtained. A variable-temperature ^{13}C NMR study was undertaken. For **1–3** intramolecular polytopal rearrangement is observed for the three carbonyl groups on each of the two ruthenium atoms along the doubly bridged edge; coalescence temperature = −40 °C. In **6**, by contrast, all the carbonyl groups equilibrate at temperatures above −80 °C. Complexes **2**, **5**, and **6** have been characterized by X-ray crystal structure determinations at −158 °C. Diffraction data were collected with a Syntex $P\bar{1}$ automated diffractometer using graphite-monochromated Mo Kα radiation. All non-hydrogen atoms were located and refined by standard Fourier and least-squares techniques. Molecule **2** crystallizes in the $P2_1/c$ space group with a = 8.297 (2) Å, b = 11.549 (5) Å, c = 34.957 (5) Å, β = 93.62 (2)°, V = 3343 (2) Å^3, Z = 8, and ρ_{calcd} = 2.75 g cm^{-3}. The final discrepancy indices are R_F = 4.8% and R_{wF} = 6.1% for 4528 independent reflections having $I > 3\sigma(I)$ in the range $0° < 2\theta < 50°$. The crystallographic asymmetric unit consists of two independent molecules (A and B). These each contain a triangular arrangement of ruthenium atoms; for each molecule two ruthenium atoms are mutually bridged by one bromine and one hydrogen atom although the latter was located only in molecule A. Each bridged ruthenium atom is associated with three carbonyl groups, while the unique ruthenium atom is linked to four such ligands. Ruthenium–carbon distances for the carbonyl groups trans to the bromine (average trans Ru–C = 1.866 (13) Å) are the shortest known for complexes of the type $Ru_3(\mu\text{-H},\mu\text{-X})(CO)_{10}$ where X = COMe, $CNMe_2$, SCH_2CO_2H, NO, $OCNMe_2$, $C_7H_4S_2N$, and CO (in the anion $Ru_3(\mu\text{-H},\mu\text{-CO})(CO)_{10}^-$). Molecule **5** crystallizes in the $Pna2_1$ space group with a = 23.854 (6) Å, b = 8.295 (3) Å, c = 9.231 (3) Å, V = 1826 (1) Å^3, Z = 4, and ρ_{calcd} = 2.63 g cm^{-3}. The final discrepancy indices are R_F = 2.5% and R_{wF} = 3.3% for 4528 independent reflections having $I > 3\sigma(I)$ in the range $0° < 2\theta < 55°$. The three ruthenium atoms form an isosceles triangle; Ru(1)–Ru(2) = 2.858 (1) Å, Ru(1)–Ru(3) = 2.870 (1) Å, and Ru(2)–Ru(3) = 3.301 (1) Å. The Ru(2)–Ru(3) separation represents zero bond order. Ruthenium atoms 2 and 3 are symmetrically bridged by two iodine atoms and are associated with three carbonyl groups, while the unique ruthenium atom is linked to four such ligands. Ruthenium–carbon distances for the carbonyl groups trans to the iodine are shortest; the average trans Ru–C = 1.874 (9) Å. Molecule **6** crystallizes in the $I2/a$ space group with a = 12.810 (4) Å, b = 15.685 (4) Å, c = 16.208 (5) Å, β = 99.65 (4)°, V = 3210 (2) Å^3, Z = 8, and ρ_{calcd} = 2.83 g cm^{-3}. The final discrepancy indices are R_F = 3.6% and R_{wF} = 5.3% for 2519 independent reflections having $I > 3\sigma(I)$ in the range $0° < 2\theta < 50°$. The three ruthenium atoms form a nearly isosceles triangle; Ru(1)–R(2) = 2.754 (1) Å, Ru(1)–Ru(3) = 2.747 (2) Å, and Ru(2)–Ru(3) = 2.898 (1) Å. Ruthenium atoms 2 and 3 are believed to be bridged by a hydrogen atom although this was not located directly. The iodine atom forms a cap on the ruthenium triangle; distances to the ruthenium atoms are Ru(1)–I(1) = 2.677 (1) Å, Ru(2)–I(1) = 2.693 (2) Å, and Ru(3)–I(1) = 2.684 (1) Å. Angles subtended by iodine, ruthenium, and trans carbonyl carbon atoms deviate significantly from ideal octahedral geometry as a result of the stereochemical constraints imposed by the presence of the face-bridged iodine and the edge-bridged hydrogen atoms: I(1)–Ru(1)–C(13) = 148.9 (22)°, I(1)–Ru(2)–C(22) = 151.65 (22)°, and I(1)–Ru(3)–C(33) = 155.81 (24)°.

Introduction

The complex $Ru_3(\mu\text{-H},\mu\text{-Br})(CO)_{10}$ was first discovered as a byproduct in the synthesis of $Ru_3(\mu\text{-H},\mu\text{-O=CMe})(CO)_{10}$ starting from $Ru_3(CO)_{12}$ and LiMe stabilized by LiBr.[1] In contrast to the triosmium hydrido–halogen complexes,[2,3] those of ruthenium, $Ru_3(\mu\text{-H},\mu\text{-X})(CO)_{10}$ (X = Cl (**1**), Br (**2**), I (**3**)) and $Ru_3(\mu\text{-H},\mu_3\text{-I})(CO)_9$ (**6**) had not as yet been reported. On the other hand, it was known that halides, in particular iodide salts, are promoters in syngas conversions catalyzed by $Ru_3(CO)_{12}$.[4,5] We thus undertook a study that led to the hydrido–halogen complexes **1–3**, the isolation of the byproducts $Ru_3(\mu\text{-X})_2(CO)_{10}$ (X = Br (**4**), I (**5**)), and the discovery of the reversible interconversion of **3** to $Ru_3(\mu\text{-H},\mu_3\text{-I})(CO)_9$ (**6**).[1] In separate contributions[6] we have described the reaction of the hydrido–halogen triruthenium complexes with ethylene and carbon monoxide. These complexes thus provide ruthenium cluster chemistry analogous to that observed for osmium through the reactive cluster $H_2Os_3(CO)_{10}$ whose ruthenium analogue has not been isolated or observed. In connection with our syntheses we also determined the crystal and molecular structures of **2**, **5**, and **6**; the results are reported below.

Chart I. Summary of Complexes (and Isolated Yields) Observed in the Reaction Sequence: (i) $Ru_3(CO)_{12}$ + Me_3NO + LiX; (ii) $HBF_4 \cdot 2Et_2O$

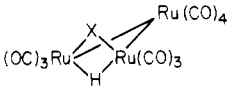

1, X = Cl (35%)
2, X = Br (33%)
3, X = I (20%)

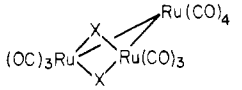

4, X = Br (5%)
5, X = I (5%)

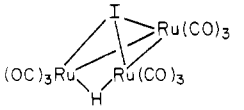

6 (35%)

Results

The derivatives isolated in this work are summarized in Chart I. Complexes **4** and **5** were isolated as byproducts in this work, but a route to these in higher yield is available as mentioned in the Experimental Section.

(1) Boag, N. M.; Kampe, C. E.; Lin, Y. C.; Kaesz, H. D. *Inorg. Chem.* **1982**, *21*, 1708.
(2) Deeming, A. J.; Hasso, S. *J. Organomet. Chem.* **1976**, *114*, 313.
(3) Johnson, B. F. G.; Lewis, J. Pippard, D. *J. Chem. Soc., Dalton Trans.* **1981**, 407.
(4) Dombek, B. D. *J. Am. Chem. Soc.* **1981**, *103*, 6508.
(5) Knifton, J. F. *J. Am. Chem. Soc.* **1981**, *103*, 3959.
(6) (a) Preliminary communication: Kampe, C. E.; Boag, N. M.; Kaesz, H. D. *J. Am. Chem. Soc.* **1983**, *105*, 2896. (b) Full paper: Kampe, C. E.; Boag, N. M.; Kaesz, H. D. *J. Mol. Catal.* **1983**, *21*, 297.

0020-1669/84/1323-1390$01.50/0

Table I. Infrared and ^1H NMR Data for New Compounds

compd	ν(CO),[a] cm^{-1}	δ(Ru-H)[b]
1	2113 vw, 2077 s, 2070 s, 2034 sh, 2030 vs, 1997 w	−13.89
2	2112 vw, 2076 s, 2069 s, 2030 vs, 2024 sh, 1996 w	−14.39
3	2109 vw, 2072 s, 2066 s, 2028 vs, 2021 sh, 1995 w	−15.02
4	2113 w, 2084 s, 2075 s, 2033 vs, 2024 sh, 1998 w	
5	2108 w, 2077 s, 2069 m, 2030 vs, 2019 w, 1996 w	
6	2096 w, 2070 vs, 2049 vs, 2017 vs, 2002 w, 1988 w	−17.67

[a] Hexane solution. [b] $CDCl_3$.

Table II. $\{^1H\}^{13}C$ NMR Data for New Compounds[a]

compd	δ(CO)
1	203.2 (1), 202.0 (1), 198.7 (2),[b] 191.7 (2),[b] 191.5 (2), 181.0 (2)[b]
2	204.6 (1), 203.4 (1), 198.4 (2),[b] 191.3 (4),[b,c] 181.3 (2)[b]
3	206.8 (1), 206.1 (1), 197.4 (2),[b] 191.2 (2), 190.7 (2),[b] 182.7 (2)[b]

[a] Only a single resonance is observed for **6** at 191.2 ppm at temperatures above −80 °C; $CDCl_3$, relative to tetramethylsilane. [b] These resonances start to broaden at −40 °C; due to thermal instability of the complexes, temperatures could not be raised above 35 °C to obtain coalescence of these peaks into an averaged signal. [c] The nonfluxional carbonyl group contribution to this resonance does not broaden; see text.

Spectroscopic data for the new compounds are presented in Tables I and II; representative spectra are deposited in the supplementary material.

IR. The absorptions in the carbonyl region of the triruthenium complexes **1–3** show one less maximum compared to what is observed for the analogous triosmium complexes.[2] In the latter, a well-resolved maximum is seen around 2013–2015 cm^{-1}; the corresponding absorption in the triruthenium derivatives must be buried under the nearby strong absorption at 2030 or 2028 cm^{-1}. A similar situation is seen for complexes **4** and **5** and their triosmium analogues.[7] This parallels the spectra of the parent carbonyls in which the maxima of four medium or strong bands are seen for $Os_3(CO)_{12}$ but only three for $Ru_3(CO)_{12}$.[8] A closer correspondence in maxima, on the other hand, is found for **6** and its triosmium analogue.[3]

^{1}H NMR. The resonances for the triruthenium complexes are uniformly at lower field (range: −13.9 to −15.0 ppm) than the resonances in the corresponding triosmium complexes (range: −14.16 to −15.24 ppm).

^{13}C NMR. The greatest difference between the sets of derivatives of these two metals is seen in the ^{13}C NMR spectra. In the triosmium analogues of **1–3**, the only exchange process that could be seen to temperatures around 70 °C is the equlibration of carbonyl groups on the unique (tetracarbonyl) osmium atom.[9] The triruthenium complexes show evidence of a different exchange; see Table II.

For **1** and **3** the limiting spectrum at −40 °C consists of six signals fully consistent with the expected geometry; see discussion of structure, below; signals of intensity 1 are assigned to axial carbonyl groups of the $Ru(CO)_4$ fragment.

For **2** the limiting spectrum at −40 °C consists of five signals; the peak of relative intensity 4 must contain a coincidentally isochronous pair of carbonyl signals. In a proton-coupled spectrum at −40 °C this signal is broadened, indicating that it contains the carbon resonances of the carbonyl groups trans to the bridging hydrogen.[9] At temperatures above −40 °C both signals of intensity 2 are seen to broaden and at 30 °C to disappear into the base line. At the same time the peak of intensity 4 is reduced to intensity 2 and three signals of relative intensity 1:1:2 remain. A comparable process is observed for complexes **1** and **3**; see Table II. Six carbonyl groups in each **1–3** are thus seen to exchange; these groups we assign as those coordinated to the ruthenium atoms on the doubly bridged edge.

In complex **6** all the carbonyl groups are observed to equilibrate above −80 °C.

Experimental Section

General Procedures. All inert-air manipulations were performed under nitrogen in standard Schlenk-type glassware. Chromatographic separations and handling of neutral complexes can be done in air without observable decomposition. Solvents were degassed by bubbling nitrogen through them for 5–10 min.

Reagents. Solvents and reagents were of commercial reagent grade and were used without further purification unless otherwise noted. THF was freshly distilled before use from sodium benzophenone ketyl solution under nitrogen. $Ru_3(CO)_{12}$ was obtained from Strem Chemicals Inc. Trimethylamine *N*-oxide was sublimed before use, although it was found that use of the dihydrate resulted in no noticeable decrease in yields as noted by other workers.[3]

Instrumentation. Carbonyl infrared spectra in the region 1500–2250 cm^{-1} were recorded on a Nicolet MX-1 Fourier transform spectrometer using cells equipped with CaF_2 windows. ^1H NMR spectra were run at 32 °C on a Bruker WM-200 spectrometer and are referenced to tetramethylsilane. ^{13}C NMR spectra were obtained in the temperature range −80 to +35 °C on a JEOL FX90Q spectrometer and are referenced to internal tetramethylsilane. Elemental analyses were carried out by Schwarzkopf Microanalytical Laboratories.

Synthesis of $Ru_3(\mu\text{-}H,\mu\text{-}X)_{10}$ (X = Cl (1), Br (2)). $Ru_3(CO)_{12}$ (1.00 g, 1.56 mmol) and the corresponding alkali halide (0.272 g of LiBr or 0.133 g of LiCl, 3.13 mmol) are dissolved in 500 mL of THF in a 1-L Schlenk flask which is connected to a mineral oil bubbler under a nitrogen atmosphere. This orange-yellow solution is cooled to 0 °C in an ice bath and stirred. Next, a solution of trimethylamine *N*-oxide (0.248 g, 3.44 mmol) in 10 mL of CH_2Cl_2 is added; the solution quickly becomes deep red. The reaction is monitored by the disappearnace of the absorbance at 2061 cm^{-1} in the IR region corresponding to $Ru_3(CO)_{12}$ and is complete within 10 min. This solution is then titrated with $HBF_4 \cdot 2Et_2O$ until absorptions corresponding to the product (2075 cm^{-1} for **1** and 2077 cm^{-1} for **2**) maximize and low-energy absorptions between 1990 and 1600 cm^{-1} disappear. The solution is then warmed to room temperature, and solvent is removed under vacuum. The residue is extracted first with 10 mL of petroleum ether and then with 5 mL of 1:1 petroleum ether/dichloromethane. Combined extracts are reduced to low volume (ca. 4 mL) and chromatographed on a silica gel (70–230 mesh) column (2.5 cm^2 × 25 cm) using petroleum ether as eluant. The first fast-moving orange-red band is product, **1** or **2**, and a small quantity of $Ru_3(CO)_{12}$. (In the workup of **2**, this band is followed closely by a faint yellow band identified as $Ru_3(\mu\text{-}Br)_2(CO)_{10}$ (**4**) (60 mg, 0.080 mmol, 5%).[10] This, in turn, is followed by a well-resolved, slow-moving, deep red band corresponding to the known tetranuclear cluster $H_2Ru_4(CO)_{13}$[11] (0.25–0.35 g, 20–30%). Solvent from the solution containing the first fraction is again removed under vacuum, and a minimum amount (ca. 3 mL) of degassed spectral grade pentane is used to selectively dissolve **1** or **2**, leaving behind the less soluble orange-yellow $Ru_3(CO)_{12}$. Recrystallization from pentane yields analytically pure **1** (0.340 g, 35%) or **2** (0.320 g, 33%). Anal. Calcd for $Ru_3C_{10}O_{10}HBr$ (**1**): C, 18.083; H, 0.1518; Br, 12.030. Found:

(7) Deeming, A. J.; Johnson, B. F. G.; Lewis, J. *J. Chem. Soc. A* **1980**, 897.
(8) Battiston, G. A.; Bor, G.; Dietler, U. K.; Kettle, S. F. A.; Rossetti, R.; Sbrignadello, G.; Stanghellini, P. L. *Inorg. Chem.* **1980**, *19*, 1961.
(9) Bryan, E. G.; Forster, A.; Johnson, B. F. G.; Lewis, J.; Matheson, T. W. *J. Chem. Soc., Dalton Trans.* **1977**, 196.
(10) Compounds **4** and **5** formed in the syntheses of **2** and **3**, respectively, are identified by elemental analysis as given in the text and by the similarity of their infrared absorption spectra to those of their osmium analogues. See: Deeming, A. J.; Johnson, B. F. G.; Lewis, J. *J. Chem. Soc. A* **1970**, 897.
(11) Johnson, B. F. G.; Johnston, R. B.; Lewis, J.; Robinson, B. H.; Wilkinson, G. *J. Chem. Soc. A* **1968**, 2856.

Table III. Crystal and Intensity Collection Data for **2**, **5**, and **6**[a,b]

molecule	$Ru_3(\mu\text{-H},\mu\text{-Br})(CO)_{10}$	$Ru_3(\mu\text{-I})_2(CO)_{10}$	$Ru_3(\mu\text{-H},\mu_3\text{-I})(CO)_9$
fw	664.23	837.12	683.21
a, Å	8.897 (2)	23.854 (6)	12.810 (4)
b, Å	11.549 (5)	8.295 (3)	15.685 (4)
c, Å	34.957 (5)	9.231 (3)	16.208 (5)
β, deg	92.62 (2)	90.0	99.65 (4)
V, Å^3	3343 (2)	1826 (1)	3210 (2)
Z	8	4	8
ρ(calcd)	2.75	2.63	2.83
space group	$P2_1/c$	$Pna2_1$	$I2/a$
cryst size, mm	0.12, 0.12, 0.31	0.16, 0.16, 0.26	0.15, 0.16, 0.40
boundary faces	$0\bar{1}\bar{1}$, $0\bar{1}1$, 011, $00\bar{1}$, $\bar{1}00$, 100[f]	201, $2\bar{1}0$, $\bar{2}10$, $\bar{2}01$ 210, 210, $00\bar{1}$[g]	010, $0\bar{1}0$, 001, $00\bar{1}$ $\bar{1}01$, $\bar{1}0\bar{1}$, 100[h]
abs coeff (μ), cm^{-1}	51.92	41.21	46.76
transmission factors	0.3248–0.6624	0.3920–0.4863	0.2858–0.5084
scan rate, deg min^{-1}	3.0	6.0	12.0
scan range			
above $K\alpha_1$	0.7	1.0	1.0
below $K\alpha_2$	0.7	1.0	1.0
2θ limits, deg	50	55	50
obsrvns	$h,k,\pm l$	$h,k,\pm l$	$h,k,\pm l$
total measd data	5912	2235	2850
no. of unique data ($I_o > 3\sigma(I_o)$)	4528	2149	2519
total no. of variables	541	225	199
R[c]	0.048	0.025	0.036
R_w[d]	0.061	0.033	0.053
S[e]	1.81	1.25	1.96

[a] Temperature: 115 K. [b] Radiation source: Mo Kα (graphite monochromated) 0.7107 Å. [c] $R = \Sigma(||F_o| - |F_c||)/\Sigma|F_o|$. [d] $R_w = [\Sigma w(|F_o| - |F_c|)^2/\Sigma w|F_o|^2]^{1/2}$, $w = 1/(\sigma^2|F_o|)$. [e] Error in observation of unit wt (goodness of fit) $= [\Sigma w(|F_o| - |F_c|)^2/(N_o - N_v)]^{1/2}$, where N_o is the number of observations and N_v is the number of variables. [f] At distances (mm) of 0.0, 0.12, 0.12, 0.0, 0.0, and 0.31, respectively, from a common point. [g] At distances (mm) of 0.0, 0.0, 0.0, 0.0, 0.16, 0.16, and 0.265, respectively, from a common point. [h] At distances (mm) of 0.15, 0.0, 0.155, 0.0, 0.0, 0.155, and 0.405, respectively, from a common point.

C, 18.18; H, 0.13; Br, 12.06. Calcd for $Ru_3C_{10}C_{10}HCl$ (**2**): C, 19.380; H, 0.1626; Cl, 5.720. Found: C, 19.53; H, 0.24; Cl, 5.69.

The trace quantity of **4** prepared in the synthesis of **2** can be isolated and recrystallized. Anal. Calcd for $Ru_3C_{10}O_{10}Br_2$ (**4**): C, 16.163; Br, 21.506. Found: C, 16.10; Br, 21.53. This derivative may be obtained in higher yield by treatment of **2** (180 mg, 0.271 mmol) with 3-bromopropene (1 mL, 11.6 mmol) in hexane solution (30 mL) at 25 °C for 10 h. Yield: 191 mg, 95%.

Synthesis of $Ru_3(\mu\text{-H},\mu\text{-I})(CO)_{10}$ (3) and $Ru_3(\mu\text{-H},\mu\text{-I}_3)(CO)_9$ (6). Compound **6** is the predominant species formed under the conditions outlined for the synthesis of **1** or **2** using NaI (0.469 g, 3.13 mmol) as the nucleophile. Purification of **6** is achieved through chromatographic separation using a column 2.5 cm^2 × 35 cm (the two compounds have similar R_f values). **3** elutes ahead of **6**, both as red-orange bands, followed by a small amount of **5** (65 mg, 0.078 mmol, 5%).[10] This, in turn, is followed by a well-resolved red band corresponding to $H_2Ru_4(CO)_{13}$. Recrystallization and workup of the mother liquor yield analytically pure deep red crystals of **6**. Total yield is 0.598 g (56%). Anal. Calcd for $Ru_3C_9O_9HI$: C, 15.822; H, 0.1475; I, 18.574. Found: C, 15.78; H, 0.13; I, 18.59. **6** is converted to a solution predominantly of **3** in 5–10 min under bubbling of CO at atmospheric pressure.

To obtain **3** directly, the extraction step in the synthesis above is followed by reduction of volume under a stream of CO. Light red crystals, obtained by slowly cooling to −20 °C, are then filtered and dried. Further crops are grown from the mother liquor; total yeild is 0.590 g (53%). Anal. Calcd for $Ru_3C_{10}O_{10}HI$: C, 16.888; H, 0.1417; I, 17.843. Found: C, 17.06; H, 0.17; I, 17.72. **3** is converted to a mixture containing predominantly **6** by removing solvent under vacuum and redissolving.

The trace quantity of **5** prepared in the synthesis of **3** can be isolated and recrystallized. Anal. Calcd for $Ru_3C_{10}O_{10}I_2$ (**5**): C, 14.348; I, 30.319. Found: C, 14.99; I, 27.90. This derivative may be obtained in higher yield by treatment of **3** (100 mg, 0.141 mmol) with 3-iodopropene (1 mL, 11.6 mmol) in hexane solution (30 mL) at 25 °C for 10 h. Yield: 97 mg, 82%.

Structure Determinations of $Ru_3(\mu\text{-H},\mu\text{-Br})(CO)_{10}$ (2), $Ru_3(\mu\text{-I})_2(CO)_{10}$ (5), and $Ru_3(\mu\text{-H},\mu_3\text{-I})(CO)_9$ (6)

General Procedures. The data for all three determinations were collected on a Syntex P$\bar{1}$ automated diffractometer equipped with scintillation counter and graphite monochromator. Intensity data were collected by using the $\theta/2\theta$ scan technique with Mo Kα radiation; scan rates and scan ranges employed for each crystal are given in Table III. The background was obtained from the peak profile. Observed reflections were corrected for Lorentz and polarization effects and converted to $|F_o|$ and $\sigma(|F_o|)$ by means of the CARESS program;[12] absorption corrections were applied. All calculations for the solution and refinement of the structures were performed on a VAX 11/780 computer. Programs used for the structure determination consist in all cases of local modifications edited by Dr. C. E. Strouse and his research group.[12] Scattering factors for neutral ruthenium, iodine, bromine, oxygen, and carbon atoms were taken from Table 2.2A of ref 13 while those for hydrogen were from Stewart et al.[14] Both real ($\Delta f'$) and imaginary ($\Delta f''$) components of anomalous dispersion were included for ruthenium using the values in Table 2.3.1 of ref 13.

Crystals of **2**, **5**, and **6** were each grown from pentane at −20 °C. Details of crystal faces, instrumental orientation, and determination of unit cell parameters and space group are given in the supplementary material. Refined unit cell parameters and specifics related to collection of data at −158 °C are given in Table III. For **5**, a survey of the complete data set revealed systematic absences for reflections ($h0l$), h = odd, and ($0kl$), $k + l$ = odd, consistent with the assignment of either *Pnam* or $Pna2_1$ for the space group. Eight triangular ruthenium clusters per unit cell were estimated on consideration of the cell volume, suggesting the space group to be $Pna2_1$. The correctness of this space group assignment is indicated by the subsequent successful refinement of the structure. For **6** a survey of the complete data set showed systematic absences for reflections (hkl), $h + k + l$ = odd, and ($k0l$), h = odd, consistent with the assignment of either *Ia* or

(12) Functions and programs employed are given as follows: data reduction, CARESS, programs for control of the Syntex diffractometer orginally written by R. W. Broach (University of Wisconsin) and P. Coppens, P. Becker, and R. H. Blessing (SUNY, Buffalo); Patterson and Fourier programs, adapted from algorithms in MULTAN78, P. Main University of York, York, England); full-matrix least-squares and error analysis, ORFLS and ORFEE, W. R. Busing, K. O. Martin, and H. A. Levy (Oak Ridge National Laboratory); absorption correction, ABSN, P. Coppens; least-squares planes, MGTL, P. Gantzel and K. N. Trueblood; thermal ellipsoid plot program, ORTEP II, C. K. Johnson (Oak Ridge National Laboratory); structure factor table listings, PUBLIST, E. Hoel.

(13) "International Tables for X-ray Crystallography"; Kynoch Press: Birmingham, England, 1975; Vol. IV.

(14) Stewart, R. F.; Davidson, E. R.; Simpson, W. T. *J. Chem. Phys.* **1965**, *42*, 3175.

Table IV. Fractional Atomic Coordinates[a] of $Ru_3(\mu\text{-H},\mu\text{-Br})(CO)_{10}$

atom	x	y	z
		Molecule A	
C(11)	0.4927 (14)	0.2661 (10)	0.7622 (3)
C(12)	0.1554 (14)	0.2147 (11)	0.7673 (3)
C(13)	0.2582 (14)	0.4357 (11)	0.7439 (3)
C(14)	0.3363 (13)	0.1169 (11)	0.7093 (3)
C(21)	0.5367 (15)	0.2349 (12)	0.6578 (3)
C(22)	0.5321 (14)	0.4598 (10)	0.6861 (3)
C(23)	0.4217 (13)	0.4018 (10)	0.6055 (3)
C(31)	−0.0787 (15)	0.3199 (11)	0.6217 (3)
C(32)	−0.0812 (14)	0.3286 (12)	0.7063 (3)
C(33)	0.0162 (13)	0.1371 (12)	0.6715 (3)
O(11)	0.6013 (10)	0.2594 (8)	0.7831 (2)
O(12)	0.0770 (11)	0.1835 (8)	0.7897 (2)
O(13)	0.2419 (11)	0.5254 (7)	0.7451 (2)
O(14)	0.3627 (11)	0.0277 (8)	0.6992 (2)
O(21)	0.6310 (10)	0.1628 (8)	0.6577 (2)
O(22)	0.6096 (10)	0.5226 (8)	0.7033 (2)
O(23)	0.4482 (10)	0.4229 (8)	0.5751 (2)
O(31)	−0.1653 (11)	0.3378 (8)	0.5959 (2)
O(32)	−0.1650 (11)	0.3490 (10)	0.7300 (3)
O(33)	−0.0127 (10)	0.0431 (8)	0.6731 (2)
Br(1)	0.15870 (14)	0.50527 (10)	0.65997 (3)
Ru(1)	0.29577 (10)	0.27264 (8)	0.72905 (2)
Ru(2)	0.38712 (10)	0.35684 (8)	0.65808 (1)
Ru(3)	0.06323 (10)	0.29621 (8)	0.66786 (2)
H(1)	0.24	0.26	0.64
		Molecule B	
C(41)	0.0636 (14)	0.7872 (11)	0.6202 (3)
C(42)	−0.0366 (14)	0.3918 (12)	0.4410 (3)
C(43)	−0.2064 (13)	0.6414 (10)	0.6090 (3)
C(44)	0.0244 (14)	0.8494 (11)	0.5436 (3)
C(51)	0.1772 (14)	0.5077 (10)	0.9172 (3)
C(52)	0.3169 (13)	0.3915 (10)	0.8620 (3)
C(53)	0.5161 (15)	0.5054 (12)	0.9196 (3)
C(61)	−0.5342 (16)	0.7659 (11)	0.4886 (3)
C(62)	−0.3250 (13)	0.5747 (12)	0.5186 (3)
C(63)	−0.1995 (14)	0.7573 (10)	0.4855 (3)
O(41)	0.1495 (11)	0.8151 (8)	0.6444 (2)
O(42)	−0.0992 (10)	0.4719 (8)	0.4497 (2)
O(43)	−0.2661 (10)	0.5793 (7)	0.6281 (2)
O(44)	0.0917 (10)	0.9090 (8)	0.5250 (2)
O(51)	0.0772 (11)	0.5788 (8)	0.9167 (2)
O(52)	0.3084 (10)	0.3837 (8)	0.8295 (2)
O(53)	0.6181 (12)	0.5733 (9)	0.9196 (3)
O(61)	−0.6448 (11)	0.7846 (8)	0.4679 (2)
O(62)	−0.3094 (10)	0.4763 (7)	0.5157 (2)
O(63)	−0.1140 (11)	0.7632 (8)	0.4612 (2)
Br(2)	−0.54016 (14)	0.72998 (11)	0.57778 (3)
Ru(4)	−0.08211 (10)	0.74154 (8)	0.57737 (2)
Ru(5)	0.33824 (10)	0.39884 (8)	0.91614 (4)
Ru(6)	−0.34680 (11)	0.73822 (8)	0.52308 (2)

[a] Numbers in parentheses are the estimated standard deviations in the least significant digits; atoms are labeled according to Figure 1.

Table V. Fractional Atomic Coordinates[a] of $Ru_3(\mu\text{-I})_2(CO)_{10}$

atom	x	y	z
C(11)	0.0004 (4)	−0.2736 (9)	0.0537 (11)
C(12)	0.0918 (4)	−0.3561 (10)	−0.1389 (10)
C(13)	0.0877 (3)	−0.0461 (10)	−0.0096 (9)
C(14)	0.0847 (3)	−0.4869 (10)	0.1441 (10)
C(21)	0.0423 (3)	0.0085 (10)	0.2764 (9)
C(22)	0.1066 (4)	−0.0614 (11)	0.5379 (10)
C(23)	0.0386 (4)	−0.2912 (10)	0.3876 (11)
C(31)	0.2054 (3)	−0.1694 (10)	−0.0625 (9)
C(32)	0.2800 (4)	−0.2339 (11)	0.1758 (11)
C(33)	0.2033 (4)	−0.4652 (11)	0.0552 (11)
O(11)	−0.0457 (3)	−0.2793 (8)	0.0494 (10)
O(12)	0.0948 (3)	−0.4059 (9)	−0.2532 (8)
O(13)	0.0864 (3)	0.0803 (8)	−0.0513 (7)
O(21)	0.0090 (2)	0.0998 (7)	0.2409 (8)
O(22)	0.1106 (3)	−0.0198 (9)	−0.3470 (7)
O(23)	0.0037 (3)	−0.3786 (8)	0.4178 (9)
O(31)	0.2085 (3)	−0.1228 (9)	−0.1785 (9)
O(32)	0.3249 (3)	−0.2220 (10)	0.1993 (9)
O(33)	0.2065 (3)	−0.5935 (8)	0.0119 (8)
I(1)	0.18237 (2)	0.05038 (6)	0.24000 (9)
I(2)	0.17630 (2)	−0.37195 (7)	0.39792 (9)
Ru(1)	0.08245 (3)	−0.27188 (8)	0.05291 (10)
Ru(2)	0.09532 (3)	−0.14359 (8)	0.33836 (10)
Ru(3)	0.19938 (3)	−0.25343 (8)	0.12436 (11)

[a] Numbers in parentheses are the estimated standard deviations in the last significant digits; atoms are labeled according to Figure 2.

Table VI. Fractional Atomic Coordinates[a] of $Ru_3(\mu\text{-H},\mu_3\text{-I})(CO)_9$

atom	x	y	z
C(11)	0.7690 (6)	0.2187 (5)	0.3981 (4)
C(12)	0.7958 (5)	0.3866 (5)	0.3378 (4)
C(13)	0.9020 (6)	0.3375 (5)	0.4975 (5)
C(21)	1.0140 (6)	0.4458 (5)	0.2954 (5)
C(22)	1.1080 (6)	0.4458 (5)	0.2954 (5)
C(23)	1.2127 (6)	0.3559 (5)	0.3162 (5)
C(31)	0.9499 (7)	0.0914 (6)	0.4364 (6)
C(32)	1.1614 (6)	0.1031 (5)	0.4014 (5)
C(33)	1.0807 (6)	0.1940 (5)	0.5374 (5)
O(11)	0.7013 (4)	0.1729 (4)	0.4036 (3)
O(12)	0.7422 (4)	0.4412 (4)	0.3085 (4)
O(13)	0.9134 (4)	0.3656 (3)	0.5644 (3)
O(21)	0.9754 (5)	0.5033 (4)	0.2580 (4)
O(22)	1.1272 (4)	0.3618 (4)	0.2939 (4)
O(23)	1.2911 (4)	0.3618 (4)	0.2939 (4)
O(31)	0.8955 (5)	0.0396 (4)	0.4501 (5)
O(32)	1.2227 (5)	0.0555 (4)	0.3890 (4)
O(33)	1.1034 (5)	0.2037 (4)	0.6084 (3)
I(1)	0.96824 (3)	0.22687 (3)	0.26358 (2)
Ru(1)	0.88345 (4)	0.29494 (3)	0.38862 (3)
Ru(2)	1.07704 (4)	0.34990 (4)	0.35698 (3)
Ru(3)	1.04767 (4)	0.18062 (4)	0.42104 (3)

[a] Numbers in parentheses are the estimated standard deviations in the last significant digits; atoms are labeled according to Figure 3.

$I2/a$ for the space group. Eight triangular ruthenium clusters per unit cell were estimated on consideration of the cell volume, suggesting the space group to be $I2/a$. The correctness of this space group assignment (nonstandard setting of $C2/c$) is indicated by the subsequent successful refinement of the structure.

Solution and Refinement of the Structures. The solutions for the structures of **2** and **6** were each obtained by a straightforward application of the heavy-atom method; solution for the structure of **5** was obtained by a combination of Patterson and difference Fourier syntheses that yielded the positions for two iodine and three ruthenium atoms. Further details are given in the supplemental material. The data for all three structures were corrected for the effects of absorption (see Table III, applied to F^2). Final discrepancy indices for each of the structures are also given in Table III.

An attempt was made to find the hydrogen atoms in **2** by using a low-angle data set ($\sin\theta < 0.35$, 1071 reflections). A reasonable position for one hydrogen atom was that bridging Ru(2) and Ru(3) of one symmetry-independent molecule. This hydrogen atom, however, could not be refined. Its position is therefore reported by us to be only probable. The hydride of the second symmetry-independent molecule is believed to bridge ruthenium atoms 5 and 6 in a similar fashion. Difficulty in the detection of the low-density hydride hydrogen atoms is due in part to the rather noisy background in the difference map. The maximum peak in the final difference Fourier map was 2.8 e/Å^3, not associated with any particular feature in the structure.

An attempt to locate the hydrogen atom in **6** by using a low-angle data set ($\sin\theta < 0.35$, 563 reflections) was unsuccessful. The maximum peak in the final difference Fourier map was 1.14 e/Å^3, not associated with any particular features in the structure. Nevertheless, the hydrogen atom is believed to bridge ruthenium atoms 2 and 3 on the basis of the elongated ruthenium–ruthenium bond and the disposition of the carbonyl groups on this cluster edge.

The final atomic positions for each of the three structures are given in Tables IV, V, and VI, respectively, together with estimated standard deviations on the final least-squares correlation matrix. Thermal

Table VII. Bond Lengths (Å)[a]

	$Ru_3(\mu\text{-H},\mu\text{-Br})(CO)_{10}$[b]		
	Molecule A		
Ru(1)-Ru(2)	2.813 (1)	Br(1)-Ru(2)	2.559 (2)
Ru(1)-Ru(3)	2.802 (1)	Br(1)-Ru(3)	2.561 (2)
Ru(2)-Ru(3)	2.819 (1)	H(1)-Ru(2)	1.8
	Molecule B		
Ru(4)-Ru(5)	2.816 (1)	Br(2)-Ru(5)	2.571 (2)
Ru(4)-Ru(6)	2.811 (1)	Br(2)-Ru(6)	2.574 (1)
Ru(5)-Ru(6)	2.818 (1)	H(1)-Ru(3)	1.8
	$Ru_3(\mu\text{-I})_2(CO)_{10}$[c]		
Ru(1)-Ru(2)	2.858 (1)	I(1)-Ru(2)	2.779 (1)
Ru(1)-Ru(3)	2.870 (2)	I(1)-Ru(3)	2.767 (1)
Ru(2)-Ru(3)	3.301 (1)	I(2)-Ru(2)	2.761 (1)
		I(2)-Ru(3)	2.765 (1)
	$Ru_3(\mu\text{-H},\mu_3\text{-I})(CO)_9$[d]		
Ru(1)-Ru(2)	2.754 (1)	I(1)-Ru(1)	2.677 (1)
Ru(2)-Ru(3)	2.898 (1)	I(1)-Ru(2)	2.693 (2)
Ru(1)-Ru(3)	2.747 (2)	I(1)-Ru(3)	2.684 (1)

[a] Numbers in parentheses are the estimated standard deviations in the last significant digits. [b] Atoms are labeled according to Figure 1. [c] Atoms are labeled according to Figure 2. [d] Atoms are labeled according to Figure 3.

Table VIII. Interatomic Angles (deg) in $Ru_3(\mu\text{-H},\mu\text{-Br})(CO)_{10}$[a]

	Molecule A		
Ru(2)-Br(1)-Ru(3)	66.80 (5)	C(23)-Ru(2)-Br(1)	89.95 (33)
C(11)-Ru(1)-C(12)	91.41 (45)	C(31)-Ru(3)-C(32)	100.57 (50)
C(11)-Ru(1)-C(13)	91.72 (47)	C(31)-Ru(3)-C(33)	94.35 (50)
C(11)-Ru(1)-C(14)	90.98 (47)	C(31)-Ru(3)-Br(1)	87.33 (37)
C(21)-Ru(2)-C(22)	94.25 (48)	C(32)-Ru(3)-C(33)	90.08 (53)
C(21)-Ru(2)-C(23)	93.40 (48)	C(32)-Ru(3)-Br(1)	95.99 (41)
C(21)-Ru(2)-Br(1)	173.34 (37)	C(33)-Ru(3)-Br(1)	173.30 (34)
C(22)-Ru(2)-C(23)	101.04 (45)	Ru(2)-H(1)-Ru(3)	104.5
C(22)-Ru(2)-Br(1)	90.75 (34)		
	Molecule B		
Ru(5)-Br(2)-Ru(6)	66.42 (4)	C(52)-Ru(5)-Br(2)	93.91 (34)
C(41)-Ru(4)-C(42)	99.49 (49)	C(53)-Ru(5)-Br(2)	89.24 (38)
C(41)-Ru(4)-C(43)	92.84 (46)	C(61)-Ru(6)-C(62)	100.92 (48)
C(41)-Ru(4)-C(44)	90.57 (47)	C(61)-Ru(6)-C(63)	94.50 (51)
C(51)-Ru(5)-C(52)	91.59 (46)	C(61)-Ru(6)-Br(2)	87.42 (37)
C(51)-Ru(5)-C(53)	96.73 (52)	C(62)-Ru(6)-C(63)	89.37 (48)
C(51)-Ru(5)-Br(2)	171.37 (35)	C(62)-Ru(6)-Br(2)	95.26 (32)
C(52)-Ru(5)-C(53)	96.58 (48)	C(63)-Ru(6)-Br(2)	174.58 (36)

[a] Atoms are labeled according to Figure 1. Numbers in parentheses are the estimated standard deviations in the last significant digits.

parameters are deposited in the supplementary material. Selected interatomic distances for all three compounds are given in Table VII. A more complete listing for each compound is given in Table VIIIA–C, respectively, as supplemental data. Selected interatomic angles for the three derivatives are given as Tables VIII, IX, and X, respectively.

Discussion of the Structure of 2

The crystal consists of discrete molecular units of $Ru_3(\mu\text{-H},\mu\text{-Br})(CO)_{10}$ that are separated by distances greater than 2.8 Å, with the closest approach being between the intermolecular oxygen atoms O(22) and O(32). The complex crystallizes in the monoclinic space group $p2_1/c$ with eight molecules per unit cell. There are thus two independent molecules in the crystallographic asymmetric unit, A and B. The overall geometry and the atom-numbering system in symmetry-independent molecule A are shown in Figure 1. Numbering in symmetry-independent molecule B is described in the caption to Figure 1. The bridging hydrogen atom was located only in molecule A; its position was not refined.

Metal Triangle and Bridging Atoms. The molecule possesses approximate C_s symmetry in the crystalline state. The three ruthenium atoms of molecule A define a triangle in which one of the nonbridged ruthenium–ruthenium edges is somewhat shorter than the other nonbridged edge: Ru(1)–Ru(3) = 2.802 (1) Å, Ru(1)–Ru (2) = 2.813 (1) Å. These in turn are only slightly shorter than the bridged edge, Ru(2)–Ru(3) = 2.819

Table IX. Interatomic Angles (deg) in $Ru_3(\mu\text{-I})_2(CO)_{10}$[a]

Ru(2)-I(1)-Ru(3)	73.04 (3)	C(23)-Ru(2)-I(2)	90.49 (26)
Ru(2)-I(2)-Ru(3)	73.35 (3)	C(23)-Ru(2)-I(1)	173.41 (28)
C(12)-Ru(1)-C(11)	96.68 (37)	C(23)-Ru(2)-Ru(1)	84.43 (30)
C(12)-Ru(1)-C(13)	93.94 (35)	C(22)-Ru(2)-I(2)	87.48 (24)
C(12)-Ru(1)-C(14)	93.53 (37)	C(22)-Ru(2)-I(1)	90.19 (26)
C(12)-Ru(1)-Ru(2)	167.18 (25)	C(22)-Ru(2)-Ru(1)	177.67 (24)
C(12)-Ru(1)-Ru(3)	96.85 (25)	I(2)-Ru(2)-I(1)	86.54 (4)
C(11)-Ru(1)-C(13)	94.13 (32)	I(2)-Ru(2)-Ru(1)	90.19 (4)
C(11)-Ru(1)-C(14)	91.12 (33)	I(1)-Ru(2)-Ru(1)	89.69 (4)
C(11)-Ru(1)-Ru(2)	96.13 (28)	C(31)-Ru(3)-C(33)	91.81 (39)
C(11)-Ru(1)-Ru(3)	166.24 (29)	C(31)-Ru(3)-C(32)	96.67 (37)
C(13)-Ru(1)-C(14)	170.32 (35)	C(31)-Ru(3)-I(2)	172.89 (25)
C(13)-Ru(1)-Ru(2)	84.77 (24)	C(31)-Ru(3)-I(1)	91.59 (26)
C(13)-Ru(1)-Ru(3)	87.38 (23)	C(31)-Ru(3)-Ru(1)	83.23 (25)
C(14)-Ru(1)-Ru(2)	86.58 (27)	C(33)-Ru(3)-C(32)	96.32 (38)
C(14)-Ru(1)-Ru(3)	85.61 (24)	C(33)-Ru(3)-I(2)	89.28 (29)
Ru(2)-Ru(1)-Ru(3)	70.36 (3)	C(33)-Ru(3)-I(1)	173.66 (26)
C(21)-Ru(2)-C(23)	91.50 (33)	C(33)-Ru(3)-Ru(1)	85.40 (27)
C(21)-Ru(2)-C(22)	98.26 (34)	C(32)-Ru(3)-I(2)	90.19 (28)
C(21)-Ru(2)-I(2)	173.71 (24)	C(32)-Ru(3)-I(1)	88.59 (27)
C(21)-Ru(2)-I(1)	90.86 (23)	C(32)-Ru(3)-Ru(1)	178.28 (27)
C(21)-Ru(2)-Ru(1)	84.07 (25)	I(2)-Ru(3)-I(1)	86.70 (4)
C(23)-Ru(2)-C(22)	95.57 (40)	I(2)-Ru(3)-Ru(1)	89.85 (3)

[a] Atoms are labeled according to Figure 2. Numbers in parentheses are the estimated standard deviations in the last significant digits.

Table X. Interatomic Angles (deg) in $Ru_3(\mu\text{-H},\mu_3\text{-I})(CO)_9$[a]

Ru(1)-I(1)-Ru(2)	61.71 (3)	C(21)-Ru(2)-Ru(1)	91.66 (22)
Ru(1)-I(1)-Ru(3)	61.65 (4)	C(21)-Ru(2)-Ru(3)	147.23 (23)
Ru(2)-I(1)-Ru(3)	65.24 (4)	C(23)-Ru(2)-Ru(3)	109.86 (22)
C(11)-Ru(1)-C(12)	95.81 (29)	I(1)-Ru(2)-Ru(1)	58.87 (4)
C(11)-Ru(1)-C(13)	97.24 (30)	I(1)-Ru(2)-Ru(3)	57.24 (3)
C(12)-Ru(1)-C(13)	96.26 (30)	Ru(1)-Ru(2)-Ru(3)	58.09 (4)
C(11)-Ru(1)-Ru(3)	98.56 (21)	C(31)-Ru(3)-C(32)	95.00 (36)
C(13)-Ru(1)-Ru(2)	95.06 (22)	C(31)-Ru(3)-Ru(1)	90.31 (26)
C(12)-Ru(1)-Ru(2)	99.54 (21)	C(31)-Ru(3)-Ru(2)	147.14 (25)
I(1)-Ru(1)-Ru(2)	59.43 (4)	C(32)-Ru(3)-Ru(2)	111.39 (24)
I(1)-Ru(1)-Ru(3)	59.31 (4)	I(1)-Ru(3)-Ru(1)	59.05 (4)
Ru(2)-Ru(1)-Ru(3)	63.59 (3)	I(1)-Ru(3)-Ru(2)	57.52 (4)
C(21)-Ru(2)-C(23)	96.17 (30)	Ru(1)-Ru(3)-Ru(2)	58.32 (4)

[a] Atoms are labeled according to Figure 3. Numbers in parentheses are the estimated standard deviations in the last significant digits.

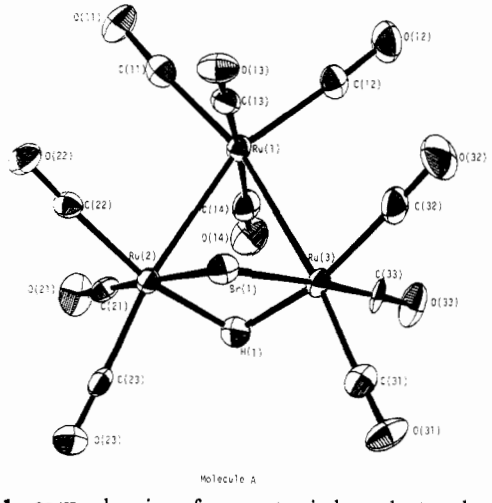

Figure 1. ORTEP drawing of symmetry-independent molecule A of $Ru_3(\mu\text{-H},\mu\text{-Br})(CO)_{10}$ (**2**) showing the atom numbering. Ellipsoids represent 50% probability surfaces. The corresponding numbering in molecule B may be seen by parallel listings in Tables VII and VIII. In molecule B the ruthenium atoms are numbered 4, 5, and 6; all other numbers are increased by 30 from those in molecule A; e.g., C(32) becomes C(62), etc.

(1) Å. In molecule B, however, the three ruthenium atoms define a more nearly equilateral triangle; nonbridged distances Ru(4)–Ru(6) = 2.811 (1) Å and Ru(4)–Ru(5) = 2.816 (1) Å are not significantly longer than the bridged distance, Ru(5)–Ru(6) = 2.818(1) Å. The average nonbridged distance for both molecules (2.810 (5) Å) is only 0.008 Å shorter than the average bridged distance (2.818 (5) Å), identical with that found for the osmium analogue $Os_3(\mu\text{-}H,\mu\text{-}Br)(CO)_{10}$.[15] These are further examples of complexes where no bond lengthening is seen with bridging hydride when this is accompanied by a second bridging atom or groups of atoms on the same edge.[16]

The bridging hydrogen atom in molecule A lies at distances from the bridged ruthenium atoms of Ru(2)–H(1) = Ru(3)–H(1) = 1.8 Å, the Ru(2)–H(1)–Ru(3) angle being 104°.

The bromine atoms are nearly equidistant from the bridged ruthenium atoms; Br(1)–Ru(2) = 2.559 (2) Å, Br(1)–Ru(3) = 2.561 (2) Å, Br(2)–Ru(6) = 2.547 (1) Å, and Br(2)–Ru(5) = 2.571 (2) Å. Corresponding angles at these bridging bromine atoms are Ru(2)–Br(1)–Ru(3) = 66.80 (5)° and Ru(5)–Br(2)–Ru(6) = 64.42 (4)°.

Ligand Enviroment around the Bridged Ruthenium Atoms and Trans Influence. Approximately octahedral coordination can be discerned around each of the bridged ruthenium atoms as defined by three carbonyl groups, a bromine atom, and a hydrogen atom. The bromine atoms are each approximately trans to a carbonyl group: Br(1)–Ru(2)–C(21) = 173.3 (4)°, Br(1)–Ru(3)–C(33) = 173.3 (3)°, Br(2)–Ru(6)–C(63) = 174.6 (4)°, Br(2)–Ru(5)–C(51) = 171.4 (4)°. A similar situation is seen for the hydrogen atom, with somewhat higher deviations from linearity: H(1)–Ru(2)–C(22) = 167° and H(1)–Ru(3)–C(32) = 165°. The remaining carbonyl groups on the bridged ruthenium atoms are approximately trans to the ruthenium atom of the $Ru(CO)_4$ fragment: C(23)–Ru(2)–Ru(1) = 171.1 (5)°, C(31)–Ru(3)–Ru(1) = 173.2 (4)°, C(61)–Ru(6)–Ru(4) = 169.2 (5)°, and C(53)–Ru(5)–Ru(4) = 171.8 (5)°. There is bonding between the bridged ruthenium atoms, but we choose not to draw in the metal–metal vector.[17] In this view of the molecule, we recognize an interesting trans influence[18] in the Ru–C distances to the carbonyl groups trans to the Br atom: Ru(2)–C(21) = 1.878 (15) Å, Ru(3)–C(33) = 1.884 (13) Å, Ru(6)–C(63) = 1.863 (12) Å, and Ru(5)–C(51) = 1.837 (12) Å. This effect has been noted for a series of similar complexes of formula $Ru_3(\mu\text{-}H,\mu\text{-}X)(CO)_{10}$, where X = COMe, $CNMe_2$, SCH_2CO_2H, NO, $OCNMe_2$, $C_7H_4S_2N$, and CO (in the anion $Ru_3(\mu\text{-}H,\mu\text{-}CO)(CO)_{10}^-$).[19] These Ru–C distances are all longer than the ones observed here, ranging from 1.968 (8) and 1.881 (9) Å for X = $OCNMe_2$ to 1.989 (7) and 1.987 (8) Å for X = COMe). These data denote a general *weakness* in the corresponding Ru–X bond and could indicate a higher reactivity to substitution at this ruthenium atom, as has been observed in recent studies in these laboratories.[20]

Other ruthenium–carbon distances in this derivative range from 1.878 (15) to 1.975 (13) Å with the longest such separations associated with carbonyl groups trans to other carbonyl groups. C–O distances range from 1.110 (13) to 1.143 (15) Å. The Ru–C–O angles are all close to linear, ranging from 174 to 179°.

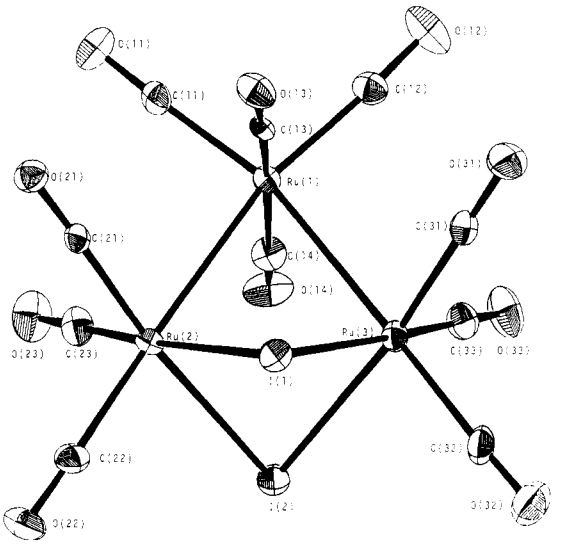

Figure 2. ORTEP drawing of $Ru_3(\mu\text{-}I)_2(CO)_{10}$ (**5**) showing the atomic number scheme. Ellipsoids represent 50% probability surfaces.

Discussion of the Structure of 5

The crystal consists of discrete molecular units of $Ru_3(\mu\text{-}I)_2(CO)_{10}$ that are separated by distances greater than 2.9 Å, with the closest approach being between intermolecular oxygen atoms O(13) and O(22). The overall geometry of the molecule and the system used for labeling the atoms are shown in Figure 2. The complex crystallizes in the monoclinic space group $Pna2_1$ with four molecules per unit cell.

Metal Triangle and Bridging Atoms. The molecule possesses approximate C_{2v} symmetry in the crystalline state. The three ruthenium atoms define an isosceles triangle: Ru(1)–Ru(2) = 2.858 (1) Å Ru(1)–Ru(3) = 2.870 (1) Å. The Ru(2)–Ru(3) separation (3.301 (1) Å) represents zero bond order. Similar Ru–Ru separations are observed in the edge-double-bridged complex $Ru_3\{\mu\text{-}NO\}_2(CO)_{10}$[21] (Å): Ru–Ru (bonding), 2.870 (1) and 2.861 (1); Ru–Ru (nonbonding, i.e. bis-NO-bridged), 3.150 (1).

In **5**, the iodine atoms are nearly equidistant from the bridged ruthenium atoms: I(1)–Ru(2) = 2.779 (1) Å, I(1)–Ru(3) = 2.767 (1) Å, I(2)–Ru(2) = 2.761 (1) Å, and I(2)–Ru(3) = 2.765 (1) Å. Corresponding angles at these bridging iodide ligands are Ru(2)–I(1)–Ru(3) = 73.04 (3)° and Ru(2)–I(2)–Ru(3) = 73.35 (3)°. By contrast, Ru–μ-N–Ru angles in $Ru_3\{\mu\text{-}NO\}_2(CO)_{10}$[21] are 101.3 (4) and 102.5 (4)°, as a result of the shorter Ru–μ-N distances, 2.03 (1) Å (average), as compared to the average Ru–μ-I distance in **5** of 2.768 (1) Å; see above.

Ligand Environment around the Bridged Ruthenium Atoms and Trans Influence. Approximately octahedral coordination can be discerned around each of the bridged ruthenium atoms as defined by three carbonyl groups and two iodine atoms. The iodine atoms are each approximately trans to a carbonyl group: I(1)–Ru(2)–C(21) = 173.71 (24)°, I(1)–Ru(3)–C(31) = 173.66 (26)°, I(2)–Ru(2)–C(21) = 173.71 (24)°, I(2)–Ru(3)–C(31) = 172.89 (25)°. In $Ru_3\{\mu\text{-}NO\}_2(CO)_{10}$[21] the corresponding features N–Ru–C_{trans} are in the range of 163.7 (4)–166.2 (4)°, owing to smaller Ru–μ-N distances as compared to the Ru–μ-I distances in **5**; see above.

The remaining carbonyl groups on the bridged ruthenium atoms in **5** are approxmately trans to the ruthenium atom of

(15) Churchill, M. R.; Lashewycz, R. A. *Inorg. Chem.* **1979**, *18*, 3261.
(16) Broach, R. W.; Williams, J. *Inorg. Chem.* **1979**, *18*, 314.
(17) We omit the convential vector between metal atoms of the doubly bridged edge of the metal triangle because we believe that this representation better reflects the octahedral coordination around the metal atoms in question.
(18) Pidcock, A.; Richards, R. E.; Venanzi, L. M.; *J. Chem. Soc. A* **1966**, 170.
(19) Bruce, M. I. "Comprehensive Organometallic Chemistry"; Pergamon Press: New York, 1982; Vol IV, p 846.
(20) "Activation of Triruthenium or Triosmium Cluster Complexes by Nucleophiles: Proceedings of the 2nd China-Japan-USA Symposium on Organometallic and Inorganic Chemistry"; Huang, Y., Teo, B.-K., Eds; Plenum Press: New York, in press.
(21) Norton, J. R.; Collman, J. P.; Dolcetti, G.; Robinson, W. T. *Inorg. Chem.* **1972**, *11*, 382–388.

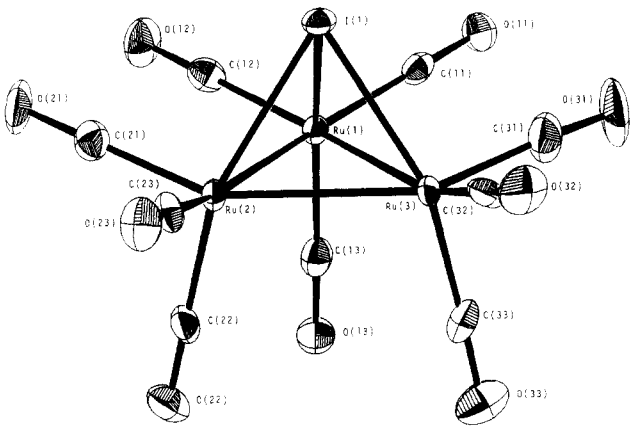

Figure 3. ORTEP drawing of $Ru_3(\mu\text{-}H,\mu_3\text{-}I)(CO)_9$ (**6**) showing the atomic numbering scheme. Ellipsoids represent 50% probability surfaces. The hydrogen atom is believed to bridge the Ru(2)–Ru(3) edge; see text.

the $Ru(CO)_4$ fragment: C(22)–Ru(2)–Ru(1) = 177.67 (24)°, C(32)–Ru(3)–Ru(1) = 178.28 (27)°. In $Ru_3\{\mu\text{-}NO\}_2(CO)_{10}$[21] the corresponding angles are 170.7 (4) and 169.3 (4)°.

As with the other structures in the present work, a trans influence[18] may be seen in the Ru–C distances to the carbonyl groups trans to the halogen atom in **5**: Ru(2)–C(23) = 1.881 (9) Å, Ru(2)–C(21) = 1.876 (8) Å, Ru(3)–C(31) = 1.866 (9) Å, and Ru(3)–C(33) = 1.871 (10)Å.

Other ruthenium to carbonyl group carbon distances in **5** range from 1.917 (9) to 1.988 (9) Å, the longest associated with carbonyl groups trans to other carbonyl groups. C–O distances range from 1.097 (11) to 1.144 (10) Å. The Ru–C–O angles are all close to linear, ranging from 174 to 179°.

Discussion of the Structure of 6

The crystal structure consists of discrete molecular units of $Ru_3(\mu\text{-}H,\mu_3\text{-}I)(CO)_9$ that are separated by distances greater than 3.1 Å with the closest approach being between intermolecular oxygen atoms O(23) and O(33). The overall geometry of the molecule and the system used for labeling the atoms are shown in Figure 3. The complex crystallizes in the monoclinic space group $I2/a$ with eight molecules per unit cell.

Metal Triangle and Bridging Atoms. The molecule possesses approximate C_s symmetry in the crystalline state. The metal framework consists of a nearly isosceles triangle containing three $Ru(CO)_3$ groups: Ru(1)–Ru(2) = 2.754 (1) Å, Ru(1)–Ru(3) = 2.742 (2) Å, and Ru(2)–Ru(3) = 2.898 (1) Å. The latter distance is significantly longer than the other two, probably due to the presence of a bridging hydrogen atom that was not located (see below).

The iodine atom caps the triruthenium face: Ru(1)–I(1) = 2.677 (1) Å, Ru(2)–I(1) = 2.693 (2) Å, and Ru(3)–I(1) = 2.684 (1) Å. The corresponding Ru–I–Ru bond angles fall in the range 62–65° (see Table X). This is the first structure study of a triruthenium cluster triply bridged by a halide ligand. A face-bridged osmium analogue of **4** is known, $Os_3(\mu\text{-}H,\mu_3\text{-}I)(CO)_9$; its structure has been inferred from spectroscopic evidence.[3] To our knowledge, the only other crystallographically determined complexes tridentate halogen ligands are the cubane-like structures $L_4M_4X_4$ where M = Cu[22a] or Ag[22b] and X = Cl, Br, or I. Triruthenium clusters capped by a single carbon,[23] nitrogen,[24] oxygen,[25] sulfur,[26] or phosphorus[27] atom have been structurally characterized.

Chart II. Designation of Carbonyl Groups for Table XI

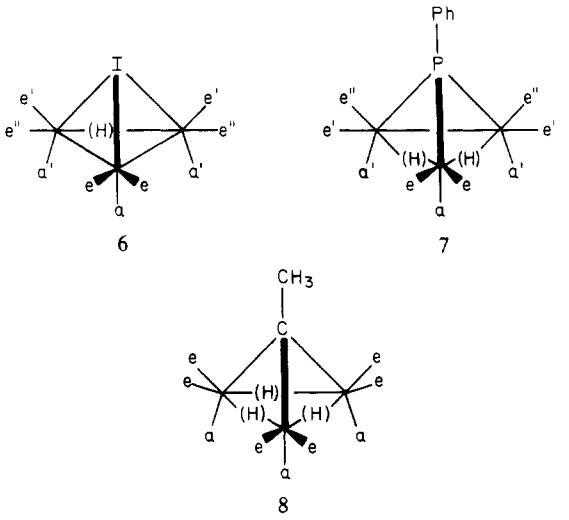

The hydrogen atom observed in the ^1H NMR spectrum was not located in difference maps. Its position may be inferred from the lengthened separation in Ru(2)–Ru(3) and the fact that equatorial carbonyls bend away from this edge of the metal triangle, namely Ru(2)–Ru(3)–C(32) = 111.39 (24)° and Ru(3)–Ru(2)–C(23) = 109.86 (22)° compared to the average of 96.9 (2)° for the other cis Ru–Ru–CO angles in this molecule.

Trans Influence in the Coordination around the Ruthenium Atoms. Ruthenium to carbonyl carbon atom distances range from 1.866 (8) to 1.964 (8) Å. Ru–C separations associated with carbonyl groups approximately trans to the Ru(2)–Ru(1) and Ru(3)–Ru(1) vectors are the longest: Ru(2)–C(23) = 1.962 (8) Å and Ru(3)–C(32) = 1.964 (8) Å. Ru–C separations trans to the halogen (as in the structures of **2** and **5**) are the shortest: Ru(1)–C(13) = 1.866 (8) Å, Ru(2)–C(22) = 1.878 (7) Å, and Ru(3)–C(33) = 1.874 (8) Å. The Ru–C–O groups are all nearly linear, with values ranging from 176 to 180°.

Effects of Edge-Bridging and Face-Capping Atoms on the Coordination Geometry around the Metal Triangle. The cis C–Ru–C angles within each of the $Ru(CO)_3$ groups in **6** fall in the range 90–101°, suggesting an octahedral framework on each metal. The metal–metal vectors however must depart from such octahedral axes due to the geometrical constraints of the metal triangle. The angles of the metal–metal vectors to each of the two carbonyl groups in an approximately trans position on each metal are Ru(2)–Ru(1)–C(11) = 159.13 (21)°, Ru(3)–Ru(1)–C(12) = 160.67 (21)°, Ru(1)–Ru(2)–C(23) = 162.51 (21)°, and Ru(1)–Ru(3)–C(32) = 159.76 (22)°.

For the capping iodine atom there is a large deviation from the octahedral axes approximated by the other bonded atoms. If we draw a normal to the trimetal plane at each metal atom, the axial carbonyl groups lie very close to this axis while the capping iodine atom is bent 37° away. The axial carbonyl groups are identified in Chart II, in which are also diagrammed the related structures $Ru_3(\mu\text{-}H)_2(\mu_3\text{-}PPh)(CO)_9$[28] (**7**) and $Ru_3(\mu\text{-}H)_3(\mu_3\text{-}CCH_3)(CO)_9$[24] (**8**). The angles of the axial carbonyl groups to their projection onto the trimetal plane in each of these structures are summarized in Table XI. The angle between the carbon atoms of each of the axial carbonyl

(22) (a) See for example; Churchill, M. R.; Youngs, W. J. *Inorg. Chem.* **1979**, *18*, 1133 and references therein. (b) See for example: Teo, B.-K.; Calabrese, J. C. *Ibid.* **1976**, *15*, 2467 and references therein.
(23) Sheldrick, G. M.; Yesinowski, J. P. *J. Chem. Soc., Dalton Trans.* **1975**, 873.
(24) Sappa, E.; Milone, L. *J. Organomet. Chem.* **1973**, *61*, 383.
(25) Lavigne, G.; Lugan, N.; Bonnet, J.-J. *Nouv. J. Chim.* **1981**, *5*, 423.
(26) Merlino, S.; Montagnoli, G. *Acta Crystallogr., Sect. B* **1968**, *B24*, 424.
(27) Iwasaki, F.; Mays, M. J.; Raithby, P. R.; Taylor, P. L.; Wheatley, P. J. *J. Organomet. Chem.* **1981**, *213*, 185.
(28) (a) Teo, B.-K.; Hall, M. B.; Fenske, R. F.; Dahl, L. F.; *J. Organomet. Chem.* **1974**, *70*, 413. (b) Mason, R.; Mingos, D. M. P. *Ibid.* **1973**, *50*, 53. (c) Kostic, N. M.; Fenske, R. F.; *Inorg. Chem.* **1983**, *22*, 666.

Table XI. Disposition of Carbonyl Groups Relative to the Trimetal Plane for $Ru_3(\mu\text{-}H,\mu_3\text{-}I)(CO)_9$ (6), $Ru_3(\mu\text{-}H)_2(\mu_3\text{-}PPh)(CO)_9$ (7),[27] and $Ru_3(\mu\text{-}H)_3(\mu_3\text{-}CCH_3)(CO)_9$ (8)[23]

	angle,[b] deg		
CO group[a]	6	7	8
e	9.8	28.5	31.1[c]
	11.3	25.9	29.7[c]
e′	13.3	27.2	
	18.2	23.0	
e″	13.4	13.4	
	10.3	12.0	
a	84.2	61.7	55.4
			55.7[c]
a′	77.7	70.3	
	76.1	71.9	

[a] Carbonyl groups are labeled according to Chart II. [b] Angle of the C-Ru vector of the CO group to its projection onto the trimetal plane. [c] Two of each of this type of CO group in the molecule.

groups to the capping iodine atom in **6** deviate significantly from 180°: I(1)–Ru(1)–C(13) = 148.91 (2)°, I(1)–Ru(2)–C(22) = 151.65 (22)°, and I(1)–Ru(3)–C(33) = 155.81 (24)°.

Departure of the capping iodine atom from the octahedral axes around each of the metal centers is seen to effect the disposition of equatorial carbonyl groups relative to the trimetal plane. These are tilted out of the trimetal plane some 10–18° toward the capping atom. The values observed in this work and compared to some other structures with the similarly capped ruthenium triangles shown in Chart II are also given in Table XI. Three types of equatorial carbonyl groups may be discerned in the comparison structures shown in Chart II: type e in which positions trans and cis to the metal–metal vectors are identical, i.e. either both unaccompanied by bridging hydrogen or both bridged by hydrogen; type e′ trans to an unbridged metal–metal vector and cis to a hydrogen-bridged metal–metal vector; and type e″, with trans and cis vectors reversed from that of type e′.

Equatorial CO groups located trans to a hydrogen-bridged metal–metal vector are bent farther out of the trimetal plane toward the capping atom as summarized by the data in Table XI. The axial CO group at such metal centers appears closer to 180° to the capping atom; see I(1)–Ru(2)–C(22) and I-(1)–Ru(3)–C(33) mentioned above. For the capped triruthenium complex **7** containing *two* bridging hydrides, the trans X–Ru–C(O) system at the metal center associated with both hydrogen bridges is even closer to linear; e.g., P–Ru–CO_{ax} = 160.7 (6)°. For comparison, the trans P–Ru–C angles at Ru atoms associated with only one hydrogen atom are 146.5 (6) and 145.7 (7)°, respectively.[28] For **8**, in which each metal–metal edge is bridged by a hydride ligand, idealized octahedral geometry around the metal atoms is also approached more closely. The relevant trans C–Ru–CO_{ax} angles are 162.1 (3) and 162.8 (6)°.

For the tricarbonyl groups adjacent to one unbridged and one H-bridged edge of the cluster, the different geometrical requirements of the equatorial groups lead to a small rotation of the tricarbonyl group around the axis defined by the metal atom and the centroid of the three CO groups.

Summary and Conclusions

There are two features to be noted in the three structures determined in this study. The first is the metal–metal separations, which uniformly reflect bond orders one would assign to achieve a closed shell around each metal atom. Counting the bridging hydrogen in **2** as a one-electron donor and the bridging bromine atom as a three-electron donor, we arrive at a metal–metal bond order of 1.[28] Indeed all three Ru–Ru separations in this derivative (see Table VII) fall within a narrow range consistent with this description. In **5**, the edge bridged by two halogen atoms contains no net bond order between the bridged metal atoms and is thus significantly longer than the unbridged metal–metal separations. In **6**, the triply bridging iodine atom as a five-electron donor and the bridging hydrogen atom as a one-electron donor replace three carbonyls from the parent cluster ($Ru_3(CO)_{12}$). This leaves a net single bond between each of the bridged metal atoms whose separations reflect this assignment. There is dissimilarity in the metal–metal separations due to the presence of the hydrogen atom (not located) along one of the edges.

The second noteworthy point is the correlation between a structural feature common to all three derivatives studied in this work and a reactivity pattern observed so far for **2** in studies under way.[20] The influence of bridging halogen in all three derivatives in this work is to strengthen attachment of carbonyl groups bonded in the trans position (see Discussion). Studies in progress on **2** indicate that substitution by phosphorus ligand occurs at ambient temperature, i.e. more rapidly than in the parent $Ru_3(CO)_{12}$. The product obtained contains the phosphorus ligand attached to the metal atom in a position cis to the halogen atom.[20] Thus the mode of reactivity must derive from a *kinetic* cis labilization.[29] Complex **2** is also reactive toward ethylene at ambient temperature, yielding an acyl halide complex.[6] Again, initial substitution for this process is believed to occur at a metal atom to which a halogen is bonded. Extrapolating to the other derivatives, enhanced reactivity in processes that require substitution as a first step may thus also be anticipated.

Acknowledgment. This work was supported by a grant from the National Science Foundation (CHE-79-08406) and an SERC Fellowship to N.M.B. Major instruments used in this work were purchased with support as follows: Syntex diffractometer, NSF Grant GP 28248; Bruker WM-200 spectrometer, NSF Grant CHE-76-05926.

Registry No. **1**, 85220-74-2; **2**, 85220-73-1; **3**, 85220-75-3; **4**, 89303-06-0; **5**, 89303-07-1; **6**, 80800-58-4; $Ru_3(CO)_{12}$, 15243-33-1; trimethylamine *N*-oxide, 1184-78-7; 3-bromopropene, 106-95-6; 3-iodopropene, 556-56-9.

Supplementary Material Available: Infrared spectra in the carbonyl stretching region for compounds **1–6** (Figures 4–9) and for **2**, **5**, and **6**, respectively, details of data collection and structure solution and refinement, listings of anisotropic thermal parameters (Table XII) and observed and calculated structure factor amplitudes (Table XIII–XV), full listings of interatomic distances (Tables VIIA–C), and packing diagrams (Figures 10–12) (63 pages). Ordering information is given on any current masthead page.

(29) Atwood, J. D.; Brown, T. L. *J. Am. Chem. Soc.* **1976**, *98*, 3160.